Charge transfer and multiple density waves in the rare earth tellurides

A. Banerjee,[1] Yejun Feng,[1,2] D. M. Silevitch,[1] Jiyang Wang,[1] J. C. Lang,[2] H.-H. Kuo,[3,4] I. R. Fisher,[4,5] and T. F. Rosenbaum[1,*]

[1]*The James Franck Institute and Department of Physics, The University of Chicago, Chicago, Illinois 60637, USA*

[2]*The Advanced Photon Source, Argonne National Laboratory, Argonne, Illinois 60439, USA*

[3]*Department of Materials Science and Engineering, Stanford University, Stanford, California 94305, USA*

[4]*The Stanford Institute for Materials and Energy Sciences, SLAC National Accelerator Laboratory, Menlo Park, California 94025, USA*

[5]*Department of Applied Physics, Stanford University, Stanford, California 94305, USA*

(Received 17 February 2013; revised manuscript received 9 April 2013; published 16 April 2013)

We use high-resolution synchrotron x-ray diffraction to uncover a second, low-temperature, charge density wave (CDW) in $TbTe_3$. Its $T_{c2} = 41.0 \pm 0.4$ K is the lowest discovered so far in the rare earth telluride series. The CDW wave vectors of the high temperature and low temperature states differ significantly and evolve in opposite directions with temperature, indicating that the two nested Fermi surfaces are separated and the CDWs coexist independently. Both the in-plane and out-of-plane correlation lengths are robust, implying that the density waves on different Te layers are well coupled through the TbTe layers. Finally, we rule out any low-temperature CDW in $GdTe_3$ for temperatures above 8 K, an energy scale sufficiently low to make pressure tuning of incipient CDW order a realistic possibility.

DOI: 10.1103/PhysRevB.87.155131 PACS number(s): 71.45.Lr, 74.70.Xa, 61.05.cp, 74.62.Fj

I. INTRODUCTION

Coexistence and competition between charge, spin, and superconducting instabilities depend vitally on the nature of the Fermi surface. Potential ground states can be tuned classically via thermal fluctuations and quantum mechanically via doping, pressure, and magnetic field, as observed in metal-insulator,[1] itinerant antiferromagnet,[2] and heavy fermion[3] materials. For charge density waves (CDWs), the instability classically arises due to a phonon-mediated interaction between electron states on matched patches of the Fermi surface, a phenomenon known as nesting, though recent *ab initio* calculations for prototypical CDW systems have questioned the role played by Fermi surface nesting.[4] Most physical realizations of nesting exist in solids with large anisotropy so as to allow lower dimensional features to develop at the Fermi surface. The layered metal-chalcogenide family has served as the historical prototype for a rich catalog of low-dimensional charge-density-wave phenomena.[5–15] The rare earth tritelluride RTe_3 series (R = La to Tm)[10,13,14,16–26] has emerged more recently as materials with extremely pliable Fermi surfaces[11] that permit multiple long-wavelength distortions, from CDW to magnetic order to superconductivity, separated by orders of magnitude in their energy scales.[22]

The RTe_3 compounds have an orthorhombic structure (space group *Cmcm*, #63), with a lattice essentially consisting of stacked double Te layers alternating with single corrugated RTe layers. This forms a unit cell with a large anisotropy between $a \approx c \approx 4.3$ Å and $b \approx 25.5$ Å [Fig. 1(a)]. The Fermi surface projected onto the a^*-c^* reciprocal space plane[17] potentially can support two degenerate CDWs along the a and c axes, respectively [Fig. 1(b)], if the lattice is tetragonal. However, this a-c degeneracy is naturally broken with slightly different a- and c-axis lattice constants, which at 100 K is approximately $(c\text{-}a) = 0.015 \pm 0.005$ Å and is independent of the choice of rare earth element.[13] Typically, only one CDW is observed along the c axis.[10,13]

Recently, a second CDW state was discovered in some members of the RTe_3 family for R = Tm, Er, Ho, and Dy at ambient pressure.[14] Although $TbTe_3$ is the nearest neighbor to $DyTe_3$ in the RTe_3 series, previous x-ray diffraction and electrical transport experiments at ambient pressure[14] as well as pump-probe spectroscopy[20] did not reveal a second CDW in this material. Using single crystal x-ray diffraction at insertion device beam lines with extremely high sensitivity, we have discovered and probed a second CDW in $TbTe_3$ for $T < 41$ K at ambient pressure. This is so far the CDW state with the lowest transition temperature in the RTe_3 family. We characterize the temperature dependence of the CDW wave vector and the CDW diffraction intensity. Both the a-axis lattice constant and the CDW order parameter indicate a continuous phase transition for the low temperature CDW in $TbTe_3$. Although the formation of the CDW was previously postulated to arise solely from the two-dimensional p_x and p_z orbitals of Te layers within the a-c plane,[16,26,27] our results indicate that changes in the strength and wave vectors of the CDW, as well as the existence of a second CDW in various RTe_3 compounds, need to take into account charge transfer between the RTe and Te layers as the b-axis lattice constant shrinks with changing rare earth element. We believe that this charge transfer effect might similarly be responsible for influencing the CDW states in both $La(Te_{1-x}Sb_x)_2$[11] and pressure-tuned $LaTe_3$.[21] A similar search for a second CDW in the rare-earth telluride $GdTe_3$, the nearest neighbor to $TbTe_3$ and the next-nearest neighbor to $DyTe_3$, did not find evidence for a low-temperature phase, with the transition bounded down to $T = 8$ K. This result suggests future searches for incipient CDW order induced by pressure at $T = 0$ in $GdTe_3$.

II. EXPERIMENTAL METHODS AND RESULTS

Single crystals of $TbTe_3$ and $GdTe_3$[14,18] were attached to either Be sheets with GE 7031 vanish or copper sticks by silver epoxy at one end, and cooled down to a base temperature of 4 K in Gifford-McMahon cryostats. Single crystal x-ray diffraction was performed on a 6-circle Huber diffractometer at beamline 4-ID-D of the Advanced Photon Source, with

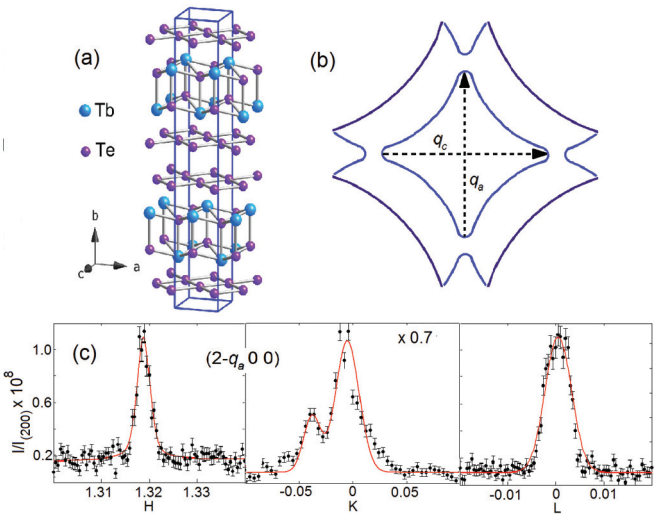

FIG. 1. (Color online) (a) Lattice structure of $TbTe_3$ with Te bilayers sandwiched between corrugated TbTe planes. (b) A general sketch of the calculated Fermi surface[14,17] showing the q_a and q_c vectors. Each drawn line of the Fermi surface would eventually split into two by the bilayer structure of the Te layers.[14] (c) *HKL* scans of CDW order $(2 - q_a, 0, 0)$. Smooth curves are a pseudo-Voigt fit in the H scan along the longitudinal direction and guides to the eye in the K and L scans. The double peak structure in the K scan is due to sample mosaicity.

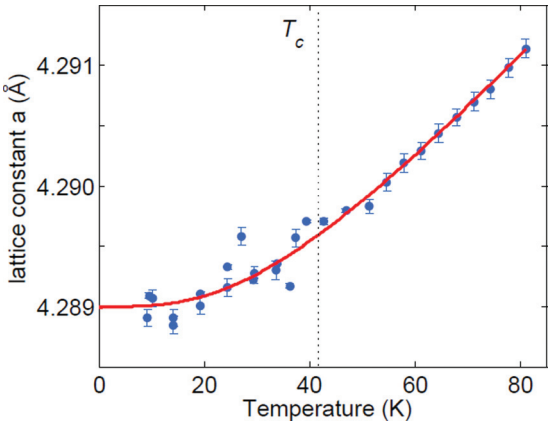

FIG. 2. (Color online) The a-axis lattice constant versus temperature demonstrates continuous behavior through the CDW transition at $T_{c2} = 41.0$ K (vertical dotted line). Fit is a two-dimensional Debye model[29] with $\Theta_D = 144 \pm 7$ K.

preliminary work carried out at beamline 6-ID-B. 20.000 keV x rays were used in a vertical diffraction geometry with a longitudinal q-resolution $\sim 1 \times 10^{-3}$ Å^{-1} (FWHM), using a set of 100 μm vertically sized detector slits on the 2θ arm 1.3 m away from the sample. Precise measurements of the lattice and c-axis CDW at $T < 10$ K yielded $a = 4.2890 \pm 0.0001$ Å, $c = 4.3067 \pm 0.0001$ Å, and $q_c = 0.7083 \pm 0.0001$ r.l.u. for $TbTe_3$, and $a = 4.2935 \pm 0.0001$ Å, $c = 4.3131 \pm 0.0001$ Å, and $q_c = 0.7121 \pm 0.0001$ r.l.u. for $GdTe_3$, consistent with values reported in the literature.[13,14]

Using bulk-sensitive hard x rays, we discovered the second CDW state in $TbTe_3$ with an incommensurate wave vector $q_a = (0.681, 0, 0)$ along the a axis. The a-axis CDW diffraction intensities are nonzero at every $(2n \pm q_a, 0,$ all) order in $TbTe_3$, in a fashion consistent with diffraction patterns of both the a-axis CDW in $ErTe_3$[14] and lattice Bragg orders $(2n, 0, 2m)$ for RTe_3 compounds.[28] We present in Fig. 1(c) representative single crystal *HKL* scans on the $(2 - q_a, 0, 0)$ order. A precise determination of the CDW wave vector $q_a = 0.6813 \pm 0.0001$ at $T = 10$ K was carried out by measuring multiple CDW peaks at $(q_a, 0, 0)$, $(2 - q_a, 0, 0)$, and $(2 - q_a, 0, 2)$, with reference to the $(2, 0, 0)$ and $(0, 0, 2)$ lattice peaks. In addition, we also observed diffraction intensity at sum peak positions of $(2 \pm q_a, 0, 2 \pm q_c)$, which was similarly observed in $ErTe_3$[14] and proves that both CDW order parameters coexist inside the same volume, instead of separating into two single-Q type domains.

We analyze first the lattice structure of $TbTe_3$ as a function of temperature from 7 to 80 K. The a-axis lattice constant was measured through the $(2, 0, 0)$ Bragg order and is presented in Fig. 2. Given that $TbTe_3$ is a layered compound, we have used a two-dimensional Debye expansion[29] to fit the lattice constant, yielding a Debye temperature $\Theta_D = 144 \pm 7$ K for data measured up to $\Theta_D/2$. This value is comparable to $\Theta_D = 161$ and 181 K obtained from the specific heat measurements in $CeTe_3$[18] and $LaTe_3$,[14] respectively. We assume a completely dispersionless b axis and an isotropic expansion in the a-c plane over this temperature range. Any dispersion will introduce a systematic error. A more accurate estimate will require measurements of all three major axes as a function of temperature. Importantly, the smooth evolution of the a-axis lattice on both sides of the CDW transition temperature T_{c2} (fixed by the order parameter in Fig. 3 and marked with a dotted line in Fig. 2) rules out any strong first order transition for the low-temperature CDW in $TbTe_3$.

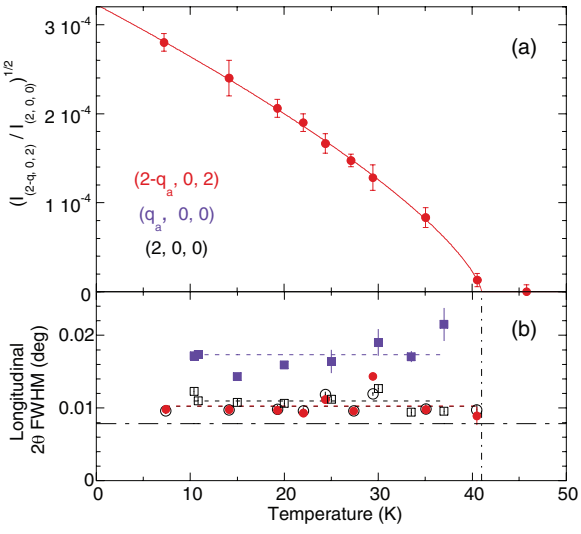

FIG. 3. (Color online) (a) The order parameter as a function of temperature. $I_{(2-q,0,2)}$ is the integrated intensity of the $(2 - q_a, 0, 2)$ peak, normalized to the integrated intensity of the $(2, 0, 0)$ Bragg peak $I_{(200)}$. (b) The FWHM of the θ-2θ scans show no broadening effects at T_{c2} within error bars on either the $(2, 0, 0)$ Bragg peak or the CDW $(q_a, 0, 0)$ and $(2 - q_a, 0, 2)$ peaks. The horizontal dot-dashed line at 0.0079° indicates our instrument resolution at the $(2, 0, 0)$ order. The vertical dot-dashed line marks the position of T_{c2} at 41.0 K.

The integrated diffraction intensity of the $(2 - q_a, 0, 2)$ CDW order provides a measure of the a-axis CDW order parameter. We plot in Fig. 3(a) the CDW order parameter so derived, normalized to the intensity of the (2, 0, 0) lattice peak. We fit the integrated intensity I to the critical form $I \sim (1 - T/T_{c2})^{2\beta}$, yielding a transition temperature $T_{c2} = 41.0 \pm 0.4$ K and a critical exponent $\beta = 0.71 \pm 0.06$. Deviations from mean field behavior also have been observed in pump-probe spectroscopic measurements of the CDW gaps in $HoTe_3$, $DyTe_3$, and $TbTe_3$.[20]

On two different parts of the sample we measured the a-axis CDW order at $(q_a, 0, 0)$ and $(2 - q_a, 0, 2)$ with a focus on the longitudinal diffraction linewidth. For both measurements, the diffraction profile at the (2, 0, 0) lattice order also was obtained for comparison. As shown in Fig. 3(b), longitudinal FWHMs of the (2, 0, 0) peak in the two cases are essentially identical, and always larger than our instrument resolution. The coherence lengths of the crystalline lattice domains are about 1700 Å and temperature independent. For the CDWs, the longitudinal FWHM of the $(2 - q_a, 0, 2)$ order does not exceed that of the lattice at all temperatures. On the other hand, the longitudinal FWHM of the $(q_a, 0, 0)$ order is always broader than that of the lattice, which may be due to weak disorder pinning of the Fukuyama-Lee-Rice type.[9,15] Unfortunately, we are unable to perform a detailed line shape study because of the relatively low counting statistics on the CDW peaks [Fig. 1(c)]. The fact that the longitudinal FWHMs of both the $(q_a, 0, 0)$ and $(2 - q_a, 0, 2)$ peaks in the ordered phase do not change appreciably at the approach to T_{c2} from below indicates that we are insensitive to any critical fluctuation effects.

III. DISCUSSION

The literature documents a long history of discussion about the fundamental origin of charge-density-wave distortions, highlighting the possible scenarios of a nesting-driven CDW and a periodic lattice distortion arising from electron-phonon coupling.[4,30,31] The complicated relationship between itinerant and local entities is also exemplified in spin density wave (SDW) materials, the spin analog of the Peierls' transition in charge systems. In Cr there exist only itinerant spins but no local moments, so the nesting nature of the SDW is unambiguous. However, to illustrate the difficulty of the problem, even in this limit density-functional-theory calculations[4] have not been able to establish the incommensurate SDW ground state.[32,33] In charge systems there always exist local positively charged ions and nested itinerant electron pairs inevitably interact with local ions through the electron-phonon coupling.[4,31] The best evidence for nesting comes from ARPES measurements. With respect to the RTe_3 series, the geometrical feature of nesting at the Fermi surface is probably the most prominent in all CDW systems.[16,23,24] Hence, we believe that the nesting nature of the CDW for $TbTe_3$ cannot be ignored. Unfortunately, our x-ray measurements cannot parse the relative roles of the two effects. We note, however, that the nested itinerant electrons still could interact cooperatively with phonons. Analogous behavior was recently identified in the pure spin system GdSi, where itinerant, nested spins interact cooperatively with local spin moments.[34]

In order to illuminate the underlying physics of the two CDW states we first review the current understanding of the band structure in RTe_3 materials. Reference 16 presents a band structure calculation for RTe_3 based on a tight binding of the atomic orbitals method and derives the Fermi surface from the in-plane p_x and p_z orbitals of the Te layer. The Fermi surface is believed to be rigid and unchanging as a function of the lattice constant c.[16] On the other hand, changing the rare earth element and hence changing c will alter the overlap integral t_{para} between parallel neighboring Te p orbitals. Across the RTe_3 series, c changes from 4.271 to 4.397 Å going from $TmRe_3$ to $LaTe_3$,[13] driving t_{para} from -1.85 to -1.70 eV.[16] This small variation leads to the strength of the electron-phonon coupling V, which directly influences the CDW gap, increasing fivefold from 0.05 to 0.27 eV[16] and the c-axis CDW transition temperature growing from 244 to over 500 K. In this picture, the change in V, rather than a change in the size of the Fermi surface, also drives the change in the CDW wave vector q_c from 0.73 to 0.69 r.l.u. due to effects based on an energy gap not centered at the Fermi surface in the presence of imperfect nesting.[16] Although Ref. 16 does not address the second CDW state, whose transition temperature varies from 41 to 186 K for $TbTe_3$ to $TmTe_3$, by the same arguments the coupling strength V should drive the energy and q scales for the a-axis CDW.

Our x-ray diffraction studies of the CDWs in both $TbTe_3$ [Fig. 1(c)] and $GdTe_3$ show sharp transverse line profiles. Hence the CDW formation has a long phase coherence length along the out-of-plane b-axis direction, implying that the CDWs on different Te layers are well coupled through the RTe layers. This experimental result points to the need to consider additional effects such as charge transfer from the direction normal to the Te planes in the two-dimensional, tight-binding rigid band model.[16] The participation of rare-earth elements in CDW formation is also evidenced by the intense resonant x-ray diffraction simultaneously observed at the CDW wave vector and the Tb $M5$ edge.[25] We note that strong transverse coupling contrasts markedly with other low-dimensional CDW systems such as $2H$-$NbSe_2$[12] and $4Hb$-$TaSe_2$,[6] which manifest broad diffraction profiles out of the plane.

Comparisons with several similarly structured RTe_3 and RTe_2 systems[11,16,17,27] help paint a fuller picture. In both families of compounds, the Te layer is a common feature and CDWs exist along a major axis. The theoretical band structure calculations for $LaTe_2$[27] mandate a charge transfer of one electron from the LaTe layer to the Te layer, and find that this charge transfer is necessary for the formation of a CDW state in the Te layer. In a band structure calculation for $LuTe_3$,[16] a one-electron charge transfer from the RTe layer to the double Te layers is assumed *a priori*. Furthermore, band structure calculations of $LuTe_2$ and $LuTe_3$[17] show qualitatively similar shapes of the Fermi surface, but the nesting wave vectors are quantitatively different. Indeed, despite the qualitative similarity of the main features of the band structure for $LaTe_2$,[17,27] LaTeSb,[27] $LaTe_3$,[16,17] and even a single Te layer[27] in linear orbital theories, the levels of the respective Fermi surfaces vary over the Te p_x and p_z bands by 1 eV. Although bands at the Fermi surface are dominantly Te p_x and p_z in nature, they appear to be susceptible to the effects of band filling from the RTe layer.

In electron-deficient Sb doping of $La(Te_{1-x}Sb_x)_2$ ($0 \leqslant x \leqslant 0.35$),[11] the experimentally observed CDW wave vector q is soft and can be varied smoothly over a wide range in reciprocal space. An increase of the q vector from 0.50 to 0.84 r.l.u. is associated with a decrease of the electron density of states in the nested bands, a band-filling effect with increasing Sb doping.[11,27] This change of q vector is similar to that of the SDW wave vector in $Cr_{1-x}V_x$ ($0 < x < 0.032$),[35] another example of increasing electron deficiency at the Fermi surface. In the RTe_3 series, the evolution of the CDW wave vector is more subtle. By either varying the rare earth constituent from $TmTe_3$ to $LaTe_3$[13] or applying pressure to $LaTe_3$,[21] it is possible to continuously change the q_c wave vector from 0.69 to 0.73 r.l.u..[13,21] Since changing the rare-earth element in RTe_3 also modifies the b-axis lattice constant,[13] this increase of q could be associated with an electron-deficient charge transfer process, similar to $La(Te_{1-x}Sb_x)_2$, through an increased separation between the RTe and Te layers from $TmTe_3$ to $LaTe_3$. We also know that the observed values of the CDW q_c vector are weakly correlated with the lattice constant c, which ranges from 4.523 to 4.417 Å in $La(Te_{1-x}Sb_x)_2$[11] and 4.397 to 4.271 Å in RTe_3.[13] Given the similarity between the band structures of $LaTe_2$[17,27] and $LuTe_3$,[16,17] this relative independence between q and c indicates that the phenomenological t_{para} might not be the only control parameter.

For SDW and CDW systems such as Cr[35–37] and $2H$-$NbSe_2$,[15] the density wave state is of a single-Q type. On the other hand, it is rather common and often energetically preferable for several CDWs to coexist over a single spatial volume and form a domain of multi-Q structure. This naturally raises issues about the independence of and interactions between the CDWs. For example, in hexagonal structured $2H$-$TaSe_2$,[8] a triple-Q CDW state is known to exist with all three CDWs having the same amplitude/strength and a single transition temperature between the incommensurate and disordered states. However, in the first-order coexistence region of the incommensurate to commensurate transition, the symmetry between three CDW states can be broken.[8] In $NbSe_3$, there is a two-CDW coexistence with different wave vectors and separate transition temperatures. It is believed that these two CDWs originate from two different chain structures in the lattice and are independent.[9] Based on the diffraction intensity, the low temperature CDW transition does not appear to affect the high temperature CDW's strength.[7] Similarly, in $4Hb$-$TaSe_2$ two CDWs with different wave vectors and transition temperatures coexist. Based on transverse line profiles, the high temperature CDW has a three-dimensional type of phase coherence across all layers, while the lower temperature CDW exists primarily within single layer of trigonal prismatic coordination.[6] Given the very different symmetry (incommensurate vs commensurate) and dimensionality (two vs three), these two CDW states are believed to be largely independent of each other.

For $TbTe_3$, the relation between the two coexisting CDW states is intriguing. Fermi surface gapping for the high temperature CDW in $TbTe_3$ is well recorded by ARPES measurements.[24] Unfortunately, no ARPES result exists for $TbTe_3$ below $T = 100$ K and the opening of a second CDW gap has not yet been visualized, which could be due to either a small CDW gap or surface dimerization effects.[19] However, in the related material $ErTe_3$, a two-gap structure on the Fermi surface is clearly observed at $T = 10$ K.[23] We note that the two gaps do not overlap nor adjoin on the Fermi surface as a finite amount of spectral weight is left between the two gapped portions.[23] In the ordered phases of $TbTe_3$, both $q(T)$ evolutions are monotonic (Fig. 4), but with opposite trends. Given that the two CDW wave vectors are very different in value [by 0.014 r.l.u. in $ErTe_3$[14] and by 0.028 r.l.u. in $TbTe_3$ (Fig. 4)], it is not surprising that the two nested portions of the Fermi surface are separated and do not compete directly for the density of states. Indeed in RTe_3 there is a natural asymmetry in the lattice structure between the a and c axes.[13] The orthorhombic distortion, which originates from a gliding plane between the two Te layers, is small but essentially constant. At $T = 100$ K, the difference (c-a) is 0.015 ± 0.005 Å and is independent of the choice of rare earth element from La ($Z = 57$) to Tm ($Z = 69$).[13]

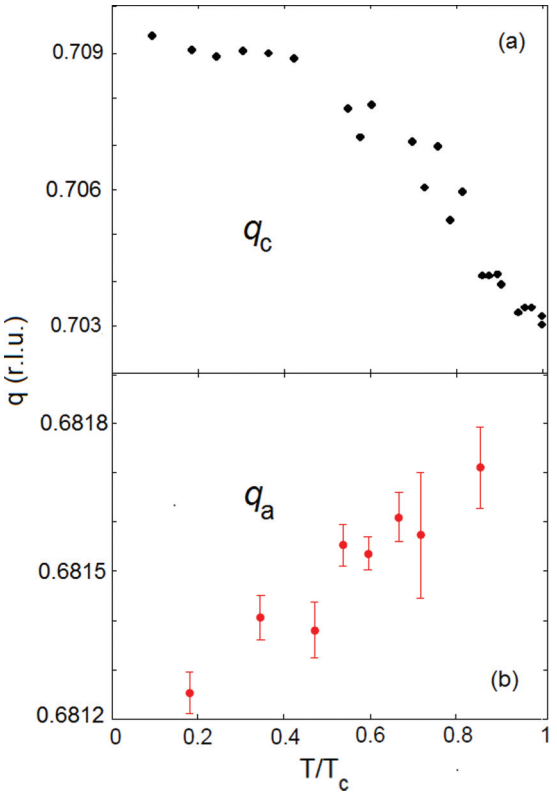

FIG. 4. (Color online) The evolution of the CDW q vectors in $TbTe_3$ as a function of temperature normalized by the transition temperatures $T_{c1} = 336$ K and $T_{c2} = 41.0$ K for the c and a axes, respectively. (a) q_c, from Ref. 14. (b) q_a. The two q vectors have different values and opposing temperature dependencies, consistent with independent coexistence.

In multiply gapped systems, such as the coexisting CDW and superconducting states in $NbSe_2$, the two directly compete for the density of states and the amplitude modes of the CDW at higher T_c can affect the ordered state at low temperature.[38] In RTe_3 the two CDWs do not directly compete for the density of states, but an indirect interaction could be channeled through the bare electron susceptibility $\chi_0(\boldsymbol{q})$. However, as long as the nesting condition still exists on the Fermi surface after

the higher temperature CDW gap opens, the local maximum in $\chi_0(\boldsymbol{q})$ at q_a associated with the lower temperature CDW should remain. Similarly, fluctuating phonon modes around one CDW should be localized near that CDW's q vector and should not unduly influence the other given the orthogonal nature of the two CDWs and their separation in reciprocal space. Experimentally, the opening of the second CDW gap with decreasing temperature in $ErTe_3$ does not seem to affect the evolution of the first CDW's gap.[23] Finally, the two density wave states with different wave vectors in the RTe_3 materials could be tuned independently by the charge transfer effect from the various rare-earth elements. By changing the Fermi surface size with effects such as charge transfer, the relative ratio of the two nesting portions are altered and both the CDW wave vectors and transition temperatures vary accordingly.

A search for the second CDW state in $GdTe_3$ at $T = 4.3$ K produced only null results. For H scans between (2, 0, 0) and (4.5, 0, 0), we had a background noise level at 2×10^{-9} of the (2, 0, 0) peak intensity, and the counting statistics of the background (∼120 photons per reciprocal lattice point) could safely rule out any CDW signals with intensity above 4×10^{-10} of the (2, 0, 0) peak. By comparison, this sensitivity is 1/25th of the CDW intensity for $TbTe_3$ at base temperature [Fig. 1(c)]. For a Peierls-type CDW instability, there typically exists a scaling relationship $I \sim \Delta^2 \sim {T_c}^2$ between diffraction intensity I, CDW gap energy Δ, and transition temperature T_c.[35–37] Assuming that all the prefactors are similar between $GdTe_3$ and $TbTe_3$, our null result provides an upper bound of $T_{c2} = 8$ K for any potential second CDW in $GdTe_3$.

Pressure techniques traditionally have been a fruitful approach for tuning both spin and charge order in solids, and for the RTe_3 family, pressure is also effective in tuning the degree of charge transfer.[21,22] Advances in x-ray diffraction and high-pressure techniques in the last decade have allowed detailed microscopic information about correlated electron states to be obtained even under many GPa of pressure.[15,21,35–37,39] Measurements of the pressure evolution of the CDW q vectors in $TbTe_3$ would determine whether those q values approach the values seen in $ErTe_3$. Additionally, rather than using pressure to suppress the correlated electron states starting from the ordered phase,[15,21,35–37,39] it would be fruitful to examine the pressure dependence of the onset of charge order in $GdTe_3$, assuming that $T_{c2}(P = 0) = 0$. From the b-axis lattice constant difference between $TbTe_3$ and $GdTe_3$[21] and the compressibility of the b axis in $CeTe_3$ under pressure,[21] one would expect the quantum phase transition of the second CDW in $GdTe_3$ to occur for $P \sim 1$ GPa. Such a modest pressure is readily available with many types of pressure vessels such as hydrostatic piston cells. The estimated low pressure and the large sample volume that could be used with these cells would even allow *inelastic* x-ray scattering techniques to be applied for studies of quantum critical phenomena in the disordered state.

IV. CONCLUSIONS

In summary, we report the observation of an incommensurate CDW in $TbTe_3$ with a second-order phase transition at $T_{c2} = 41.0 \pm 0.4$ K, adding $TbTe_3$ to the members of the rare-earth tritelluride family with coexisting CDWs in the ground state. Using our x-ray diffraction data and comparing with previous experimental and theoretical treatments of RTe_2 and RTe_3 materials, we suggest that the evolution with both chemical and applied pressure of the CDW distortions in RTe_3 materials could involve charge transfer effects from the RTe layer to the Te layers, akin to electron deficit Sb doping in $La(Te_{1-x}Sb_x)_2$. The charge transfer would simultaneously affect both the wave vectors spanning the nested sections of the Fermi surface and the relative ratio of the two separated nesting areas, thereby changing the relative strength and transition temperatures of the two CDW states. By varying the rare-earth element, we bound the lower transition temperature for $GdTe_3$ and believe that T_{c2} goes to zero between $TbTe_3$ and $GdTe_3$. A continuous tuning of the charge transfer mechanism with modest applied pressures should induce the second CDW in $GdTe_3$ at a $T = 0$ quantum phase transition. This should allow studies of quantum critical phenomena without doping-related disorder effects.

ACKNOWLEDGMENTS

The work at the University of Chicago was supported by NSF Grant No. DMR-1206519. The work at the Advanced Photon Source, Argonne National Laboratory was supported by the US Department of Energy Basic Energy Sciences under Contract No. NE-AC02-06CH11357. The work at Stanford University was supported by the DOE, Office of Basic Energy Science, under Contract No. DE-AC02-76SF00515.

*Corresponding author: t-rosenbaum@uchicago.edu

[1] M. Imada, A. Fujimori, and Y. Tokura, Rev. Mod. Phys. **70**, 1039 (1998).
[2] R. Jaramillo, Y. Feng, J. Wang, and T. F. Rosenbaum, Proc. Nat. Acad. Sci. USA **107**, 13631 (2010).
[3] S. Friedemann *et al.*, Proc. Nat. Acad. Sci. USA **107**, 14547 (2010).
[4] M. D. Johannes and I. I. Mazin, Phys. Rev. B **77**, 165135 (2008).
[5] J. A. Wilson, F. J. Di Salvo, and S. Mahajan, Adv. Phys. **24**, 117 (1975).
[6] F. J. Di Salvo, D. E. Moncton, J. A. Wilson, and S. Mahajan, Phys. Rev. B **14**, 1543 (1976).
[7] R. M. Fleming, D. E. Moncton, and D. B. McWhan, Phys. Rev. B **18**, 5560 (1978).
[8] R. M. Fleming, D. E. Moncton, D. B. McWhan, and F. J. Di Salvo, Phys. Rev. Lett. **45**, 576 (1980).
[9] D. DiCarlo, R. E. Thorne, E. Sweetland, M. Sutton, and J. D. Brock, Phys. Rev. B **50**, 8288 (1994).
[10] E. DiMasi, M. C. Aronson, J. F. Mansfield, B. Foran, and S. Lee, Phys. Rev. B **52**, 14516 (1995).
[11] E. DiMasi, B. Foran, M. C. Aronson, and S. Lee, Phys. Rev. B **54**, 13587 (1996).
[12] C.-H. Du *et al.*, J. Phys.: Condens. Matter **12**, 5361 (2000).

[13]C. Malliakas and G. Kanatzidis, J. Am. Chem. Soc. **128**, 12612 (2006), and supplemental materials therein.
[14]N. Ru *et al*., Phys. Rev. B **77**, 035114 (2008); **77**, 249908 (2008).
[15]Y. Feng *et al*., Proc. Nat. Acad. Sci. USA **109**, 7224 (2012).
[16]V. Brouet *et al*., Phys. Rev. B **77**, 235104 (2008).
[17]J. Laverock *et al*., Phys. Rev. B **71**, 085114 (2005).
[18]N. Ru and I. R. Fisher, Phys. Rev. B **73**, 033101 (2006).
[19]A. Fang, N. Ru, I. R. Fisher, and A. Kapitulnik, Phys. Rev. Lett. **99**, 046401 (2007).
[20]R. V. Yusupov *et al*., Phys. Rev. Lett. **101**, 246402 (2008).
[21]A. Sacchetti *et al*., Phys. Rev. B **79**, 201101 (2009).
[22]J. J. Hamlin *et al*., Phys. Rev. Lett. **102**, 177002 (2009).
[23]R. G. Moore *et al*., Phys. Rev. B **81**, 073102 (2010).
[24]F. Schmitt *et al*., New J. Phys. **13**, 063022 (2011).
[25]W. S. Lee *et al*., Phys. Rev. B **85**, 155142 (2012).
[26]H. Yao *et al*., Phys. Rev. B **74**, 245126 (2006).
[27]A. Kikuchi, J. Phy. Soc. Jpn. **67**, 1308 (1998).
[28]B. K. Norling and H. Steinfink, Inorg. Chem. **5**, 1488 (1966).
[29]K. Komatsu and T. Nagamiya, J. Phys. Soc. Jpn. **6**, 438 (1951).
[30]S.-K. Chan and V. Heine, J. Phys. F: Met. Phys. **3**, 795 (1973).
[31]H.-M. Eiter *et al*., Proc. Nat. Acad. Sci. USA **110**, 64 (2013).
[32]R. Hafner, D. Spisák, R. Lorenz, and J. Hafner, Phys. Rev. B **65**, 184432 (2002).
[33]V. Vanhoof, M. Rots, and S. Cottenier, Phys. Rev. B **80**, 184420 (2009).
[34]Y. Feng *et al*., Proc. Nat. Acad. Sci. USA **110**, 3287 (2013).
[35]R. Jaramillo *et al*., Phys. Rev. B **77**, 184418 (2008).
[36]Y. Feng *et al*., Phys. Rev. Lett. **99**, 137201 (2007).
[37]R. Jaramillo *et al*., Nature (London) **459**, 405 (2009).
[38]P. B. Littlewood and C. M. Varma, Phys. Rev. Lett. **47**, 811 (1981).
[39]M. Hücker *et al*., Phys. Rev. Lett. **104**, 057004 (2010).